Plasma Sources
Science and
Technology

PAPER • **OPEN ACCESS**

Determination of the accuracy of actinometry and line ratio techniques in an O_2 glow discharge: II. Electric field measurements with Ar and Xe admixtures*

To cite this article: L Kuijpers *et al* 2026 *Plasma Sources Sci. Technol.* **35** 015010

Plasma Sources Science and Technology

OPEN ACCESS

RECEIVED
30 June 2025

REVISED
1 November 2025

ACCEPTED FOR PUBLICATION
26 November 2025

PUBLISHED
16 January 2026

PAPER

Determination of the accuracy of actinometry and line ratio techniques in an O_2 glow discharge: II. Electric field measurements with Ar and Xe admixtures*

L Kuijpers[1,2,**], E Baratte[3], O Guaitella[3], J-P Booth[3], V Guerra[4], M C M van de Sanden[1,2] and T Silva[4,**]

[1] Department of Applied Physics, Eindhoven Institute for Renewable Energy Systems, Eindhoven University of Technology, Eindhoven, The Netherlands
[2] Dutch Institute For Fundamental Energy Research, De Zaale 20, 5612 AJ Eindhoven, The Netherlands
[3] LPP, CNRS, École Polytechnique, Sorbonne Université, Université Paris-Saclay, IP-Paris 91128 Palaiseau, France
[4] Instituto de Plasmas e Fusão Nuclear, Instituto Superior Técnico,Universidade de Lisboa 1049-001 Lisboa, Portugal
* Supplementary Information available: Tabulated data for the ratio of the excitation rate coefficients in figure 10.
**Authors to whom any correspondence should be addressed.

E-mail: l.kuijpers@tue.nl and tiago.p.silva@tecnico.ulisboa.pt

Keywords: line ratio method, optical emission spectroscopy, reduced electric field, CRDS, actinometry, O2 plasma, glow discharge

Supplementary material for this article is available online

Abstract

A line-ratio method for determining the reduced electric field is benchmarked against independent measurements from electrostatic probes and cavity ring-down spectroscopy. The method is applied to oxygen DC glow discharges with trace admixtures of argon and xenon. A corona model incorporating fluorescence quenching by heavy species is used to simulate the emission, with electron-impact excitation rates calculated using the LisbOn KInetics Boltzmann solver. The excitation cross sections and quenching coefficients are those proposed and validated for actinometry in part one of this combined study (Baratte *et al* 2025 *Plasma Sources Sci. Technol.*). The reduced electric field is determined over a pressure range of 0.55 to 5 Torr (at 40 mA) and a current range of 15 to 50 mA (at 5 Torr). Consistent agreement with measured emission line intensities is achieved when applying a correction factor of $\kappa_{c,Ar} = 3 \pm 0.5$ to the excitation cross sections for the argon lines at 750 nm and 811 nm. With this correction, the reduced electric field values obtained from the line-ratio method are in good agreement with direct measurements. A comparison of different line ratios is presented, showing that the best performance is achieved using the ratio of the Ar 750 nm and Xe 828 nm lines. This ratio is particularly sensitive to changes in the electron energy distribution function, due to the large difference in excitation thresholds, while remaining independent of the knowledge of species densities.

1. Introduction

For optimal utilization of low temperature plasma in its numerous applications (e.g. electrification of chemical processes [2, 3], semiconductor processing [4, 5], medicine [6], and many more [7]) a clear understanding of discharge processes and the underlying physics is required. To this purpose, it is invaluable to probe discharge parameters such as the gas or vibrational temperatures, species densities, ionization degrees and electron temperatures. Knowledge of the electron energy distribution function (EEDF), which determines the electron kinetics, is of paramount importance.

In DC glow discharges for a given gas composition, the EEDF is determined by the reduced electric field, E/N, where E is the electric field and N the gas number density. If E/N and the complete cross-section set of the gas are known, then the EEDF can be readily calculated over a wide range of conditions using freely available software [8–10]. In low pressure DC glow discharges the electric field, E, can be measured directly from the potential difference between high-impedance floating electrostatic probes

[11–14], but such a simple technique can not be used in non-homogeneous or high pressure plasmas. Alternatively, E can be measured using more complex techniques, for example by electric field induced second harmonic generation, but the complexity of this diagnostic limits practicality, and the weak signal makes it inapplicable to lower gas pressures [15–18]. In order to determine E/N from E, the gas number density, N, must also be determined. Often an ideal gas is assumed, therefore the pressure and gas temperature must be determined. Note that the pressure is generally externally controlled, while the gas temperature can be measured by a plethora of ways, often based on optical emission from the discharge [19, 20] by fitting of rotational emission bands, where the rotational temperature is often assumed to be in equilibrium with the translational temperature [21, 22], or through Doppler line broadening in laser spectroscopic techniques. Probing the EEDF can also be done in several ways, but these are often intrusive, complex or require expensive equipment. Langmuir probes can be used, but require the insertion of a physical probe in the discharge. Furthermore, the interpretation of the signal becomes complex if the sheath is collisional. Thompson scattering can only be applied for high ionization degrees, and requires costly equipment. Fitting of spectral features like Bremsstrahlung is dependent on absolute intensity calibrations [23]. Therefore, development of a simple non-intrusive method to probe the EEDF would be highly useful.

One relatively cheap and simple non-intrusive diagnostic that is often employed in gas discharges is optical emission spectroscopy (OES). Light emitted by the discharge provides information on the species and processes taking place in the plasma. Combining the spectrum with a radiative model allows for passive, non-perturbative probing of several discharge parameters. Absolute species densities can be estimated from line intensity ratios (so-called actinometry), where the ratio of emission intensities from the target species and from a trace rare gas is used to estimate the species density without knowledge of the electron density and temperature. This was described and validated in part I of this combined study [1], where the atomic oxygen density was estimated in glow discharges in 0.5–5 Torr of oxygen gas at a current of 40 mA. Specifically, traces of argon or xenon are added to determine the atomic oxygen density. In a related technique, the electron temperature can be probed using the ratio of (multiple) emission lines. Such techniques have been named the line ratio method, trace gas OES (TRG-OES), energy resolved actinometry (ERA) and state enhanced actinometry (SEA), and have been used extensively in the literature [24–28]. All of these techniques are based on measuring line intensity ratios, and their interpretation requires knowledge of basic data about the specific gases used, notably the excitation cross-sections of the levels under consideration. Unfortunately, these basic data are subject to wide dispersion in the literature, as illustrated in Part I [1]. In this work (part II), we use a discharge in which the values of the reduced field E/N and the atomic oxygen density are directly measured accurately, in order to provide strong constraints on the basic data used to deduce the reduced electric field and the O atom density from atomic lines of O, Ar and Xe. We propose a validated method to determine E/N from OES. To achieve this, we use the same DC glow discharge in pure O_2 at 0.5–5 Torr and varying current as was used for actinometry validation in part I of this combined study [1]. The reliability of the conclusions drawn is greatly enhanced by the cross-validation of the same cross-section sets for both the determination of the O atom density (part I) and the reduced electric field here (part II).

Pagnon *et al* [29] proposed an emission line ratio method to determine the reduced electric field in DC oxygen discharges at pressures in the range 0.36 to 2 Torr. In their study, the intensity ratio of two atomic oxygen triplets (at 777 nm and 844 nm) was used with an extended corona model which included dissociative excitation. The E/N values they deduced were in reasonable agreement with those obtained from direct measurement with electrostatic probes, with an error of the order of 20%. However, the validity of these results is debatable due to inconsistencies in the cross sections presented in their paper compared those given in the original source that they quote, as already discussed in part I of this work [1].

TRG-OES is a more sophisticated approach [30]. It was introduced to determine the electron temperature (rather than the reduced field) in lower-pressure radio-frequency discharges, using optical emission from up to five rare gases added in trace amounts. The measured trace gas line intensities are coupled to a collisional radiative model (CRM). The observed relative emission intensities of the different rare gases are compared with calculated values in the CRM. The different excitation energies of the different states of the multiple gases allows probing of the EEDF or (assuming a Maxwellian EEDF) the value of T_e. TRG-OES was first applied in a helical resonator plasma working at 10 mTorr Cl_2 with a power density of 0.4 W cm^{-3}, reporting an electron temperature of 2.2 ± 0.5 eV. Subsequently the method has mostly been applied to inductively coupled plasmas with pressures ranging from 1 to 90 mTorr containing Cl_2 [28, 30–38], but also for O_2 [39] and fluorocarbons [40, 41]. A review of work on this diagnostic method is given by Donnelly [28]. More recently, it has been applied to low pressure electron cyclotron resonance microwave discharges [42], to capacitively coupled plasmas up to 200 mTorr [43],

and to microwave surface wave plasmas up to 1 Torr containing O_2 [44] and Cl_2 [45]. The method generally assumes a Maxwellian EEDF, or at higher pressures a bi-Maxwellian EEDF is used with a separate electron temperature for the high energy tail of the EEDF. Various electron impact cross section sets are used in these works, most being slightly corrected experimental cross sections. An evaluation of these cross sections and their corrections is given by Donnelly [28].

Other closely related methods are SEA, and its predecessor, ERA. ERA was introduced by Greb *et al* [25] as a method to measure both the atomic oxygen density and the mean electron energy in an atmospheric pressure radio frequency (RF) plasma jet in helium with 0.5% oxygen and 0.1% trace argon gas. It has also been applied to a low pressure (0.3–0.6 Torr) oxygen RF CCP with 2% argon [26]. In the SEA method, helium emission lines are also included [27]. This was applied to an atmospheric pressure helium microplasma jet at 1 slm helium with 5 sccm O_2 and 0.5 sccm argon. By including helium emission lines, a larger range of the EEDF can be probed, due to the higher excitation energy of helium compared to argon or oxygen. However, this also requires precise knowledge of the EEDF between the very distant energy thresholds of the different excited levels.

A simplified version of both TRG-OES and ERA/SEA is the line ratio method. In this case, only two (trace gas) emission lines are used, along with a simplified CRM to calculate the electron temperature based on an assumed EEDF [46–48]. A review of the line ratio method for argon and nitrogen containing low temperature plasmas is given by Zhu and Pu [24]. It is worth mentioning that in atmospheric pressure plasmas, the ratio of N_2 and N_2^+ bands is widely used to determine the electric field. However, as for the other line ratio methods, the accuracy obtained is compromised by the lack of knowledge of the basic data, as discussed in detail by Obrusnik [49].

Several common aspects are important to all of the aforementioned techniques: the selection of appropriate emission lines, a (simple) CRM for the emitting states, the assumed shape of the EEDF, and the choice of electron-impact excitation cross sections. In this work we have drawn inspiration from the line ratio method, TRG-OES, and different actinometry schemes in order to determine E/N for a DC oxygen glow discharge. We have studied the effect of pressure (0.5–5 Torr) at 40 mA and the effect of current variation (15–40 mA) at 5 Torr. Argon (5%) and xenon (2%) are used as trace gases. We make use of a simple CRM, the corona model including quenching, with selected electron impact excitation cross sections and other input variables (i.e. quenching rates). The EEDF is calculated using the LisbOn KInetics Boltzmann solver (LoKI-B) [9, 50].

The model and input parameters are identical to those in part I of these combined works [1], where they are used to calculate emission line intensities and to determine the atomic oxygen density by actinometry in O_2–Ar and O_2–Xe discharges. In this work we extend this model and with the same input data, apply it to an O_2–Xe–Ar discharge, and adapt the method to determine the reduced electric field. The low-pressure glow discharge allows benchmarking of the atomic oxygen density against Cavity Ring Down Spectroscopy (CRDS) (part I, [1]) and reduced electric field against floating potential probe measurements (part II, presented here). Using a single constant correction factor for the argon excitation cross section, excellent agreement is found for both the atomic oxygen density and the reduced electric field. This validates both the model and the input data, i.e. the cross sections and collisional rates. Moreover, it suggests that the argon cross sections are generally underestimated in literature. These conclusions are reinforced by the consistency of the results found in parts I and II, which compare line-ratio methods with two completely independent measurement methods (CRDS and electrostatic probes) applied to the same plasma reactor.

In the remainder of the paper we will first introduce the experimental framework, after which the model and methods are highlighted. The results, and an analysis of their sensitivity to the input variables, are presented subsequently.

2. Experimental

2.1. Experimental setup

A schematic overview of the setup is given in figure 1. The Pyrex discharge tube has an inner diameter of 2 cm. The wall temperature is kept constant at 293 K by a mixture of distilled water and ethanol flowing in an outer envelope. The gas flow is controlled using mass flow controllers for oxygen and the trace gases, argon and xenon. The system is pumped by an oil-free scroll pump via a feedback-controlled throttle valve. A minimum pressure of 0.55 Torr is obtained with a total gas flow of 7.4 sccm. The maximum studied pressure (5 Torr) is limited by the ability of the power supply to maintain the plasma current. The discharge is struck between hollow electrodes placed in side-arms, supplied by a stabilized DC HV power supply through a 68 kOhm ballast resistor. The plasma is run at 15 to 50 mA DC current. Two experimental procedures are performed: a pressure scan for 0.55–5 Torr at 40 mA constant current

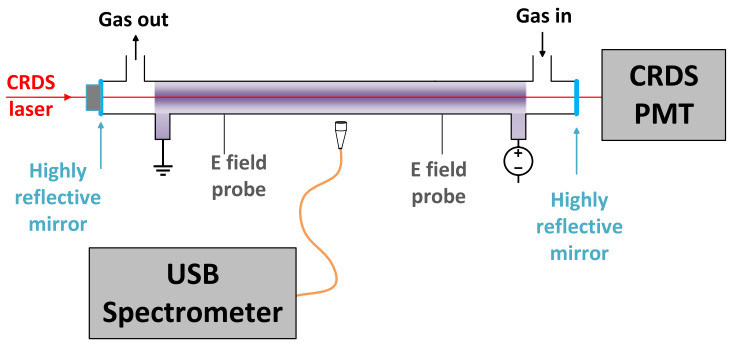

Figure 1. Schematic of the experimental setup. Pressures range from 0.55–5 Torr and discharge run at 15–50 mA DC current. Total gas flow is set at 7.4 sccm.

and a current scan of 15–50 mA at 5 Torr constant pressure. The setup is nearly identical to that in [1, 12], where it is described in more detail.

The electric field is determined by measuring the voltage drop between two floating tungsten probes embedded in the discharge tube (see figure 1). The observed values for the electric field as a function of gas pressure and discharge current are shown in figure 2. In order to calculate the EEDF for given values of E/N it is necessary to estimate the gas composition. The principal oxygen heavy species present in the discharge are ground state molecular oxygen $O_2(X^3\Sigma_g^-)$, ground state atomic oxygen $O(^3P)$, and excited metastable molecular oxygen, $O_2(a^1\Delta_g)$ [51]. The sensitivity of the estimation of E/N to the $O(^3P)$ and $O_2(a^1\Delta_g)$ populations is presented later in figure 9 and its discussion. The trace gases argon and xenon are both noble gases and do not react with the oxygen species (if we ignore metastable states). Note that achieving good repeatability of oxygen discharges is challenging, as a major loss channel of atomic oxygen is the wall recombination, and this can vary between experiments depending on the history of the surface. It is therefore generally not valid to use atomic oxygen densities from the literature and we must measure the atomic oxygen density simultaneously with the field measurements. This is achieved using the CRDS technique via the forbidden transition $O(^3P_2) \rightarrow O(^1D_2)$ (around 630 nm) as presented in [1, 12]. CRDS gives reliable absolute measurements of the atomic oxygen density $[O(^3P)]$ and additionally provides the gas temperature from the Doppler broadening of the absorption line. Values for T_g and $[O]/N$ determined by CRDS are shown in figure 2. Both the temperature and the electric field are observed to increase with pressure, as expected. The atomic oxygen fraction has a maximum at 0.75 Torr, and decreases at higher pressure. Increasing the current causes the electric field to fall slightly, while the gas temperature increases. The atomic oxygen density fraction increases with current. It should be noted the CRDS measurements are made along the central axis of the tube, due to the position of the laser beam, and will thus represent maximum values for both T_g and $[O(^3P)]/N$ [51]. More information related to the radial distributions of these quantities can be found in [11, 12, 51]. Figure 2 also shows the atomic oxygen fraction as determined by actinometry using the 750 nm argon and the 828 nm xenon emission lines with oxygen at 845 nm according to the method presented in [1], using the electron impact excitation cross sections as found in [52, 53]. Good agreement with CRDS was found using actinometry with xenon, and also with argon provided that a constant correction factor is used for the excitation cross section (introduced later in section 4.1; changing only the absolute value of the cross section, not the shape). Using argon as the actinometer without this correction factor leads to the same underestimation of the oxygen atom density as found in part I [1]. These good actinometry results obtained as a function of both both pressure and current variation give confidence in the validity of the collisional-radiative model and its use in the O_2–Xe–Ar mixture.

2.2. Optical emission spectroscopy

OES spectra are taken using an Avantes USB spectrometer (ULS4096CL-2-EVO) with a resolution of 0.5 nm. Light is collected using a collimating lens with a focal length of 5 cm to input the light into an optical fibre bundle. The optics are positioned near the discharge tube, centred axially and radially. The variation of the sensitivity with wavelength was determined by taking the spectrum of a calibrated tungsten lamp. The subsequent spectra are corrected using this factor. Note that an absolute calibration is not needed, since only the ratio of line intensities is used.

The spectra are corrected for electronic dark and background emissions. The emission intensities of each line are spectrally integrated to account for different line broadening. A typical spectrum is shown

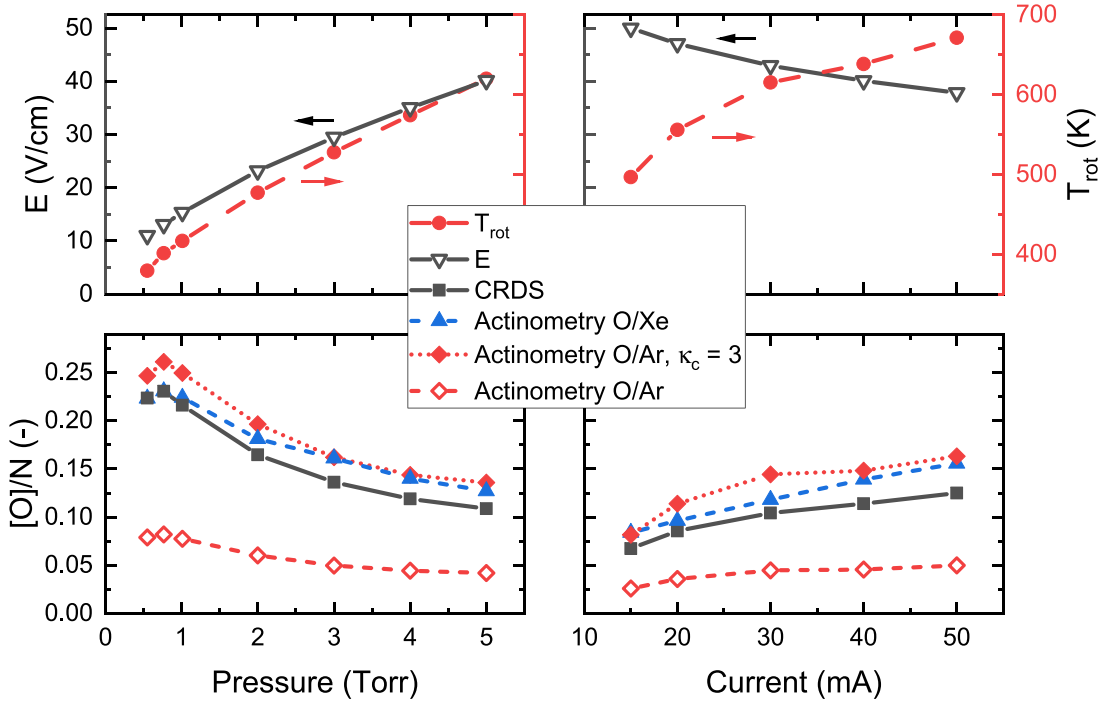

Figure 2. Experimental results for oxygen DC glow discharge with 5% argon and 2% xenon. Pressure variation at 40 mA current (left) and current variation at 5 Torr (right). T_g and [O]/N from CRDS. E from the voltage drop over two probes. Dashed lines for [O]/N show actinometry result using argon and xenon according to the method presented in part I of these combined works [1]. Dotted lines are argon actinometry results including correction factor $\kappa_c = 3$ (see section 4.1).

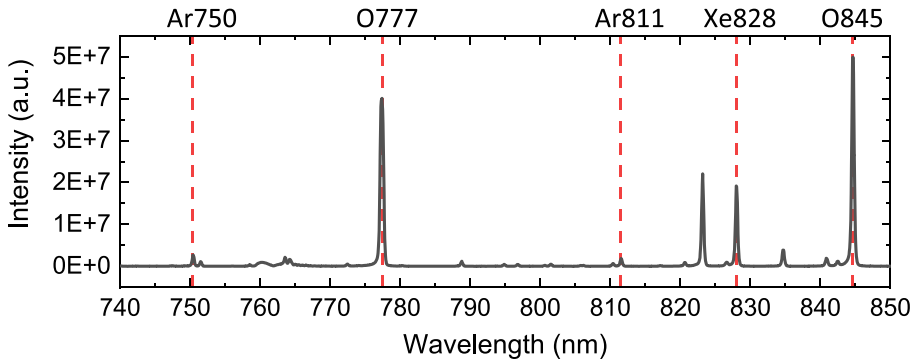

Figure 3. An OES spectrum showing the main lines considered in this work. Data from an 93% O_2 – 5% Ar – 2% Xe discharge at 1 Torr, 40 mA taken with the Avantes spectrometer. Dashed red lines indicate the atomic emission lines used in this work.

in figure 3, with dashed lines denoting the emission lines used. It is essential to use emission lines that are not convoluted with other lines. For example, argon emits at both 750 nm and 751 nm, but the resolution of our spectrometer allows for clear separation of these peaks. The spectrum shows that the xenon line at 828 nm is more intense than the argon lines, even though there is only 2% xenon in the inflow compared to 5% argon. This difference in intensity is caused by the lower threshold energy and higher excitation cross section of xenon compared to argon. It thus has a higher excitation rate and therefore will emit at higher intensity (the emission probabilities are similar for both emitting states under investigation).

3. Theory and methods

3.1. Extended corona model

The EEDF's are calculated using LoKI-B [9, 50]. This is then combined with an extended corona model including quenching to calculate the line ratios. This model was extensively validated in part I [1] in the context of atomic oxygen actinometry. In this work it is adapted to allow for the determination of E/N.

The line intensity of a transition $i \rightarrow j$ of a species X is calculated using [1, 14, 29]:

$$I_{X,i\rightarrow j} = K_X h\nu_{ij}^X k_e^X n_e a_{ij}^X [X], \tag{1}$$

where K_X is an experimental constant, dependent on the detection system, relating the observed signal intensity to the number of photons emitted, $h\nu_{ij}$ is the energy of the emitted photons, k_e^X is the electron impact excitation rate coefficient, n_e is the electron density, $[X]$ is the density of the ground state atoms, and a_{ij}^X is the effective branching factor including the quenching term:

$$a_{ij}^X = \frac{A_{ij}^X}{\Sigma_i A_i^X + \Sigma_Q k_Q^X [Q]}, \tag{2}$$

where A_{ij}^X the Einstein coefficient for the transition $i \rightarrow j$, k_Q^X is the quenching factor for species Q with density $[n_Q]$, and $\Sigma_i A_i^X$ is the sum of all transition probabilities from state i to all lower states. The rate coefficient k_e^X is calculated using:

$$k_e^X = \left(\frac{2e}{m}\right)^{\frac{1}{2}} \int_{\varepsilon_{th}}^{\infty} \sigma(\varepsilon)_i f(\varepsilon) \sqrt{\varepsilon} d\varepsilon. \tag{3}$$

Here, e is the elementary charge and m the electron mass, $\sigma(\varepsilon)_i$ is the electron excitation cross section with threshold energy ε_{th} and $f(\varepsilon)$ is the EEDF. Lastly, the electron density n_e, used to calculate the line intensities in section 4.1, is calculated from the discharge current I_0, using:

$$n_e = \frac{I_0}{\pi r^2} \frac{1}{e \cdot E \cdot \mu}, \tag{4}$$

with r the radius of the reactor, E the electric field, and μ the mobility calculated from $\mu = \mu_{red} \cdot N$, with N the gas density and μ_{red} the reduced mobility obtained from LoKI-B.

We estimate the reduced electric field, E/N, in the following way. The ratio of the intensities of emission lines A and B (from species with ground state densities [A] and [B]) is given by:

$$\frac{I_A}{I_B} = \frac{h\nu_{ij}^A}{h\nu_{ij}^B} \frac{[A]}{[B]} \frac{k_e^A}{k_e^B} \frac{a_{ij}^A}{a_{ij}^B}. \tag{5}$$

This ratio depends on the ratio of the rate coefficients k_e^A/k_e^B, which depend on the EEDF, and therefore E/N (as well as the branching factors a_{ij}^A/a_{ij}^B). It is independent of the electron density, n_e. We assume the system-dependent constant, K_X, (from (1)) is constant for all lines. The reduced electric field is then estimated by varying its value in the calculation in order to minimize the difference between the observed and calculated intensity ratios:

$$\Delta = \left| \left(\frac{I_A}{I_B}\right)_{\text{simulated}} - \left(\frac{I_A}{I_B}\right)_{\text{measured}} \right|, \tag{6}$$

as detailed in section 3.3.

3.2. Emission lines considered

The emission lines of three species are considered: atomic oxygen, argon and xenon. The lines and energy levels of these species are shown schematically in figure 4. The two oxygen electronic transitions are triplets, one emitting around 844.6 nm and the other at 777.4 nm. In this work they will be noted O845 and O777, respectively. O845 has an excitation threshold energy of $\varepsilon_{th} = 10.99$ eV, while $\varepsilon_{th} = 10.74$ eV for O777. The two argon transitions emit at 750.4 nm and 811.5 nm. They are both singlets with excitation thresholds of 13.48 eV and 13.076 eV, respectively. These lines are noted here as Ar750 and Ar811. The xenon transition emits at 828.0 nm with a threshold energy of 9.93 eV and will be noted here as Xe828. Table 1 lists the considered emission lines, the energy levels and threshold energies with the notation used in this work.

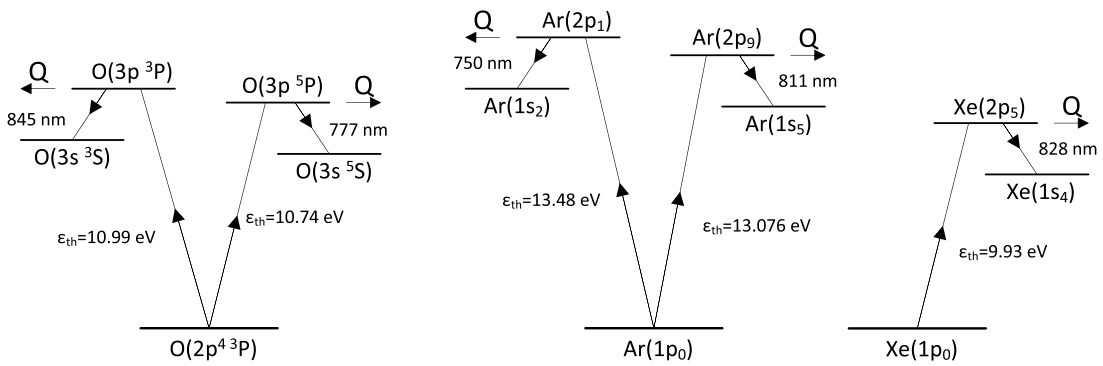

Figure 4. The extended corona model and energy levels of the lines used for the line ratio method. The levels are populated by electron impact excitation and destroyed by spontaneous emission and quenching.

Table 1. The emission lines emitting at wavelength λ_{ij}, their notation in this work, transitions (using Paschen notation for the noble gases) and threshold energies ε_{th}, electron-impact excitation cross-sections (CS), transition probabilities A_{ij} [57] and quenching rate coefficients by molecular oxygen k_Q^X.

Specie	λ_{ij} (nm)	Notation	Transition i → j	ε_{th} (eV)	CS	A_{ij} (s^{-1})	k_Q^X ($m^3\ s^{-1}$)
O	844.6	O845	O(3p ^{3}P) → O(3s ^{3}S)	10.99	[52]	3.22×10^7	9.4×10^{-16} [54]
O	777.4	O777	O(3p ^{5}P) → O(3s ^{5}S)	10.74	[52]	3.69×10^7	10.6×10^{-16} [26]
Ar	750.4	Ar750	Ar(2p1) → Ar(1s2)	13.48	[53]	4.45×10^7	7.6×10^{-16} [55]
Ar	811.5	Ar811	Ar(2p9) → Ar(1s5)	13.076	[53]	3.31×10^7	7.5×10^{-16} [55]
Xe	828.0	Xe828	Xe(2p5) → Xe(1s4)	9.93	[53]	3.69×10^7	9.8×10^{-16} [56]

3.3. Determination of E/N

The workflow for finding E/N is shown in figure 5. The experimental conditions are used as input for the calculation of the EEDF. These comprise the pressure, the gas composition (including the atomic oxygen density), the gas temperature, and the density of the metastable electronically excited state $O_2(a)$. It is important to include this state because it can comprise up to 8% of the total gas density [51]. The $O_2(a)$ densities were taken from previous experimental measurements [13], where the DC glow discharge was ignited under very similar conditions as presented here. The densities of $O(^1D)$ and $O_2(b)$ were assumed to be negligible. It should be noted that the results are not highly sensitive to the exact densities of $O(^3P)$ and $O_2(a)$. The uncertainties induced by errors in these densities are quantified in section 4.3. LoKI-B is then used to compute the EEDF, for the given discharge conditions, over a full range of E/N. From this the rate coefficients, and then the line ratios, are computed. The reduced electric field is then chosen to minimize the difference between the computed and measured line ratios in (6).

LoKI-B [9] is a MATLAB-based simulation tool which solves the two-term electron Boltzmann equation, taking as input the gas composition, pressure, gas temperature, electron density, reduced electric field (and frequency, in this case DC), and a set of electron scattering cross sections. It returns the EEDF, power density and macroscopic electron transport coefficients, including the electron mobility. The EEDF is calculated using the complete, self-consistent cross section sets for oxygen (including molecular and atomic oxygen) and argon, given in the IST-Lisbon database with LXCat [58]. For xenon the cross section set of Biagi [59] is used. A preliminary swarm analysis was performed to ensure correct calculation of the electron parameters. The reduced Townsend coefficient, reduced mobility, and reduced diffusion showed good agreement with the experimental swarm parameters (available at LXCat) at low reduced electric fields.

The method presented in this work also depends on the spontaneous emission transition probabilities, the quenching rate coefficients and the electron impact excitation cross sections. The emission transition probabilities used for the Ar, Xe and oxygen radiative transitions are taken from the NIST Atomic Spectra Database [57]. Quenching rates are taken from multiple sources. The values for quenching by molecular oxygen, which is the dominant process, are given in table 1. With the exception of Ar750 quenching by Ar, data for quenching by atomic species are not available, therefore we assume all atomic species have an equal quenching rate coefficient of $k_Q^X = 0.1\times10^{-16}\,m^3s^{-1}$ [60]. However, these processes will have a negligible effect compared to molecular oxygen. Multiple electron impact excitation cross sections are available in the literature for the emitting states. We chose the cross sections calculated by Tayal [52], for oxygen atom excitation, while the cross sections for argon and xenon are taken from

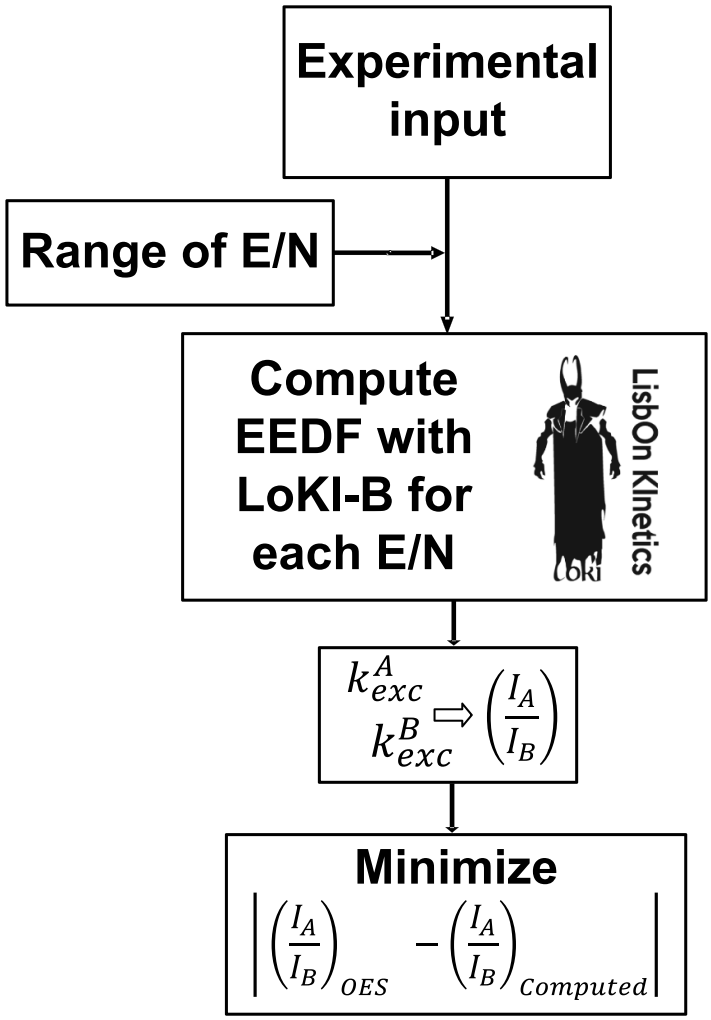

Figure 5. Workflow of the line-ratio method as presented using LoKI-B for the EEDF.

Zatsarinny [53]. All of these cross sections were obtained by calculations using the B-spline R-matrix approach. The cross sections are taken from the LXCat database [61] and plotted in figure 6. The validity of these cross sections and other input data was evaluated extensively in part I of these combined works [1], where they are shown to give the best results for the emission line intensity calculations and the atomic oxygen density determination through actinometry in O_2–Ar and O_2–Xe mixtures. The cross sections were selected based on the reproduction of the trend over E/N (through pressure variation) of the emission line intensity. Here we will assess the validity of these cross sections and the quenching rates in O_2–Ar–Xe mixtures by comparing the reduced electric field values estimated by matching the line intensity ratios to values measured directly using the floating potential probes.

4. Results

4.1. Line intensities and correction factors

The line intensities for the presented emission lines are calculated for each set of operating conditions with (1), using experimental values for the gas density and composition, in the same way as in part I [1]. Figure 7 shows the measured and simulated emission line intensity for the used lines, all normalized to the Xe828 line at 5 Torr and 40 mA. The solid lines represent the measured values, the dashed and dotted lines are simulated line intensities. The errors in the simulated line intensities come from an uncertainty in the calibration of the mass flow controllers for argon and xenon. For the xenon line there is very good agreement between experimental and simulated values. Note that, for the pressure variation, the simulated and measured values overlay nearly perfectly. The two oxygen lines show reasonable agreement between measurement and simulations. However, the experimentally-observed O777 intensity drops faster with pressure than the the 0845 line, whereas the calculated curves are almost identical

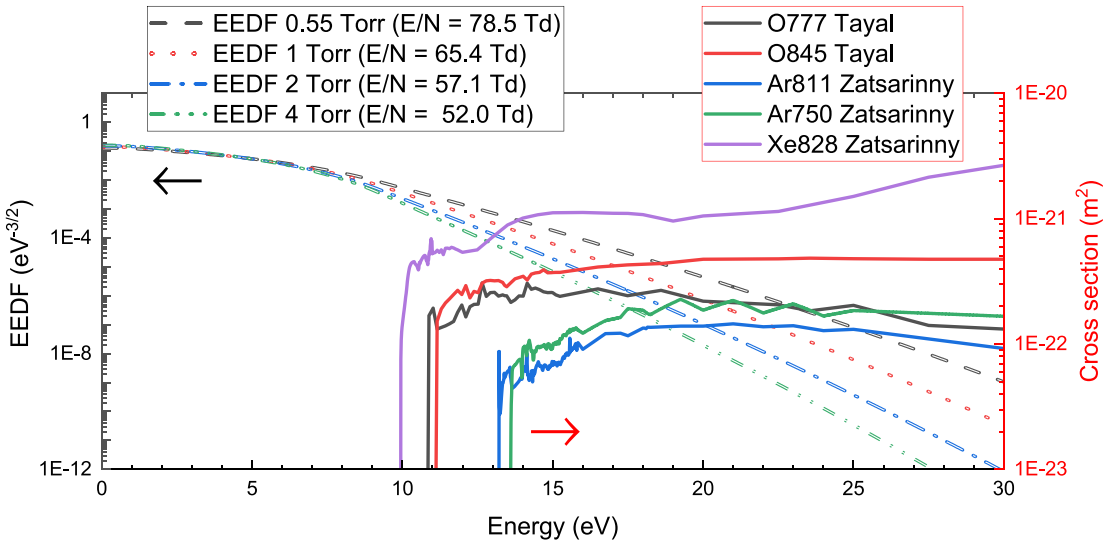

Figure 6. Calculated EEDF's for several pressure points, and the excitation cross sections used: Tayal for O777 and O845 [52], and Zatsarinny [53] for Ar750, Ar811 and Xe828. EEDF calculated by LoKI-B using previously-measured $O_2(a)$ populations [13], $O(^3P)$ densities obtained from CRDS and E/N from measured E (floating probes) with gas density N using T_g from CRDS.

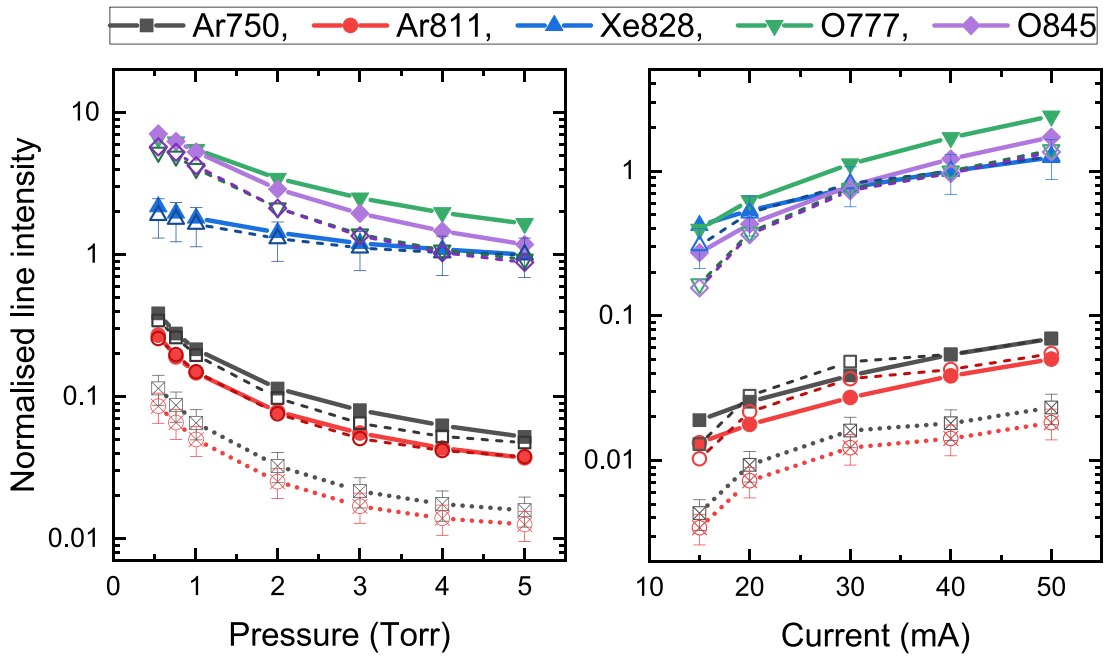

Figure 7. Normalized measured and calculated line intensities for a discharge containing 93% O_2, 5% Ar and 2% Xe. The pressure variation is measured at 40 mA current (left) and the current variation at 5 Torr (right). All line intensities are normalized to Xe828 at 5 Torr and 40 mA. Solid lines denote measured line intensities and dashed lines denote calculated results, including a correction factor of $\kappa_{c,Ar} = 3$ for argon (see (7)). The dotted lines display the calculated line intensities of the argon lines excluding this correction. The calculated line intensities are obtained using cross sections as presented in figure 6. The colours for the simulated lines are darkened to enhance contrast. Note that the simulated oxygen lines are nearly identical and mostly overlying in the figure.

for the two lines, and decrease even faster than the observations. The calculated argon line intensities are shown as dotted lines. These show a similar trend to the measurements, but the simulated intensity (normalized to the xenon line) is systematically lower than the observations by a factor of about 3.

This strong underestimation of the intensity of the Ar750 line is egregious. Therefore, we propose a correction to the rate coefficient of the emitting states in the form of a constant multiplication. This takes the form of:

$$\left(k_e^X\right)_{\text{corrected}} = \kappa_c k_e^X. \tag{7}$$

This correction factor for both argon lines is found to be $\kappa_{c,Ar} = 3 \pm 0.5$, which suggests that the cross sections used for Ar from [53] have the correct threshold energies and shapes, but not the right amplitude. In a previous comparison of the amplitude of different cross sections [62], it was found that these theoretical cross sections of [53] consistently underestimate the experimentally determined cross sections of [63] by a factor 2.5-4.7. A correction factor for xenon is not explicitly used, as it would be $\kappa_{c,Xe} = 1 \pm 0.2$. The error in the correction factor stems mainly from the error in the calculated line intensities shown in figure 7. The corrected simulated argon line intensities are also shown in figure 7 as dashed lines and are in good agreement with the measured line intensities, both in trend over pressure and current and in absolute value. The correction factor is the same for both argon lines. It is worth noting that the observed line intensities are normalized, so that the same result would be achieved by applying a correction factor of 1/3 to the oxygen and xenon data. Using absolute correction factors to correct the rate coefficients or the cross sections based on absolute emission intensities would generalize the correction factor, but is not in the scope of this work. However, the work does show good results for both actinometry and the line ratio method for a single, constant correction factor. It applies when the E/N and EEDF are varied (by pressure variation) for the relatively low energies probed in this work, justifying its use as a direct correction of the argon cross sections.

This correction factor for argon can also be used for actinometry, using the methods presented in part I of these combined works [1], and is shown in figure 2. The dashed lines are obtained without correction of the argon cross-sections, whereas the dotted line includes it. Excellent agreement is seen with the atomic oxygen fractions measured by CRDS (using either xenon or argon (with correction factor)) in terms of the trend with pressure and in absolute value.

The good agreement of the calculated line intensities, especially for xenon and argon, when implementing the correction factor, validates the use of the extended corona model. Using the measured gas composition and quenching rates from the literature [64, 65], it is found quenching by O_2 accounts for more than 92% of the destruction of argon metastables by collisions with other species. Argon metastables are therefore effectively quenched by the high density of molecular oxygen, as also shown in [66, 67]. This means that the contribution to the stepwise excitation of argon or electronic energy transfer to xenon or atomic oxygen is limited. Although the rate coefficient of quenching of argon metastables by xenon is in a similar order to that of O_2 [65], the low fraction of xenon limits the electronic energy transfer to xenon. Additionally, the process populates higher energy states and cascading into the 2p5 state is required, further limiting the potential effect on Xe828 emission [64]. For higher xenon fractions or high O_2 dissociation, the effect may not be negligible. Because the argon metastable density is unknown, a formal evaluation is out of the scope of this work. However, it should be noted that to use actinometry or the line ratio method as described in this work and part I [1], it is important to consider the validity of the CRM of each separate species and the energy transfer processes between species.

For the atomic oxygen line at 845 nm, the simulated trends with both pressure and current agree relatively well with the observations. However, for the 777 nm oxygen line the trend with pressure is in less good agreement. This suggests that the extended corona model might be less inaccurate for the O777 emitting state. Other (de)population channels have been tested. Dissociative excitation was shown to be negligible for comparable discharge conditions in other works [14, 29] and was found to account for less than 5% of the atomic oxygen density in part I of these combined works [1]. However, it might still explain the difference in agreement between simulated and measured values of O777 and O845 in figure 7, since the rate coefficient for dissociative excitation of O777 is reported to be higher than that for O845 [14]. Excitation from metastables of Ar is insignificant in the present conditions, since they are quenched efficiently by molecular and atomic oxygen at these pressures [60]. The contribution from cascading from higher levels was investigated, using the effective cascade cross section from Caplinger [60], but did not influence results significantly (a maximum change of 7% for the absolute line intensities was found). A further channel could be the population by quenching from higher levels, specifically quenching from the O(3p ^{3}P) to the O(3p ^{5}P) state. Lastly, radiation trapping through self-absorption could be occurring, as it has been shown to differ between the two emission lines [68]. The contribution of these last two (de)population channels has not been tested in this work, but is suggested as further work.

The sensitivity of the calculated line intensities to the quenching coefficients was found to be limited, requiring a factor 10 difference to significantly affect the calculated line intensities [1]. For higher pressures, quenching will be more prevalent and the accuracy of the quenching coefficients will be more important. Moreover, using temperature-independent quenching coefficients is a simplification that appears to hold for the conditions under investigation (i.e. low temperature and weak sensitivity to changes in the quenching coefficients), but it might be important to improve the precision of the quenching coefficients in other discharges with higher pressures and gas temperatures.

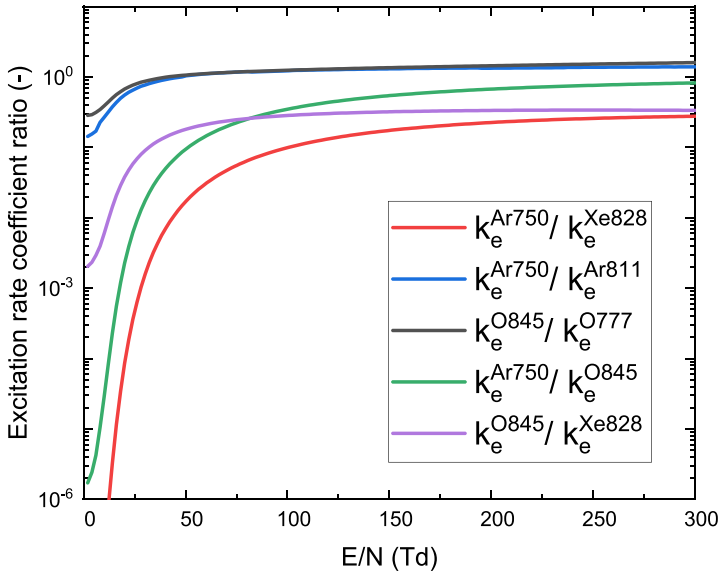

Figure 8. Excitation rate coefficient ratio plotted against the reduced electric field for multiple line ratios, using cross sections as presented in figure 6, and including the correction factor for the argon lines, $\kappa_c = 3$. Obtained at 1 Torr and 40 mA.

4.2. Determining the reduced electric field from emission spectra

The ratio of the observed emission intensity from two lines is given by (5). This depends on the ratio of the excitation rate constants, which depends on the shape of the EEDF, and therefore on reduced electric field. Therefore, in order to determine E/N from a ratio of line intensities, it is necessary to select two lines which vary in significantly different ways with E/N. Zhu and Pu [24] stated that, in order to correctly measure reduced electric field, the difference in threshold energy of the lines used should be comparable to the electron temperature, T_e. However, in the case of DC glow discharges the EEDF is far from Maxwellian. In this case, we must consider the effective electron temperature in the energy range corresponding to the excitation thresholds. In our case this corresponds to $T_e \approx 2.5$ eV. We can investigate this sensitivity to the reduced electric field by calculating the EEDF with LoKI-B. The EEDFs calculated at four values of the pressure are shown in figure 6. The relative change of the EEDF in the energy range under investigation (0–15 eV), induced by the inclusion of the trace gases, is lower than 10%. The high energy tail of the EEDF is slightly increased when the trace gases are not considered in the calculation. The reduced field, E/N, decreases as a function of pressure, as expected. The variation of the EEDF as a function of pressure (and thus E/N) directly affects the calculated line intensities. Figure 8 shows the ratio of the rate coefficients, as a function of the reduced electric field, for several combinations of lines. It shows the sensitivity to the reduced electric field of the ratio of the excitation rate coefficients for various line pairs. It is clear that the ratio of the two argon lines k_e^{Ar750}/k_e^{Ar811}, the ratio of the two oxygen lines k_e^{O845}/k_e^{O777} and the ratio of the oxygen and xenon lines k_e^{O845}/k_e^{Xe828} have low sensitivity to the reduced electric field in the area of interest, 25–100 Td (for lower E/N, these line ratios could be effective). Therefore using the two argon or two oxygen lines will provide little sensitivity to the reduced electric field in the range studied here (cf table 1). The ratios of the rate coefficients k_e^{Ar750}/k_e^{Xe828} and k_e^{Ar750}/k_e^{O845} are more sensitive, with $\Delta\epsilon_{th} = 2.5 - 3.5$ eV. However, knowledge of the ratio of the species densities is also required. Thus, using the argon–xenon line ratio Ar750/Xe828 is convenient, since the ratio of densities is known and independent of the operating conditions. If xenon is not available, the argon-oxygen line ratio could be used, but this requires measurement of the oxygen atom density. Furthermore, it is less accurate due to the less good agreement of the simulated line intensities for oxygen with the observations.

4.3. Results of the line ratio method

The reduced electric field derived from the Ar750 and Xe828 emission line ratio, using the workflow as presented in figure 5, is plotted in figure 9. The directly measured E/N is shown by solid black lines (with the gas density $N = P/k_b T_g$ using T_g from CRDS measurements). The initial results of the line ratio method are shown in the grey dashed line and reveal an overestimation of the reduced electric field by a factor of 1.5–2. This disagreement does not come as a surprise, as it has been concluded that the

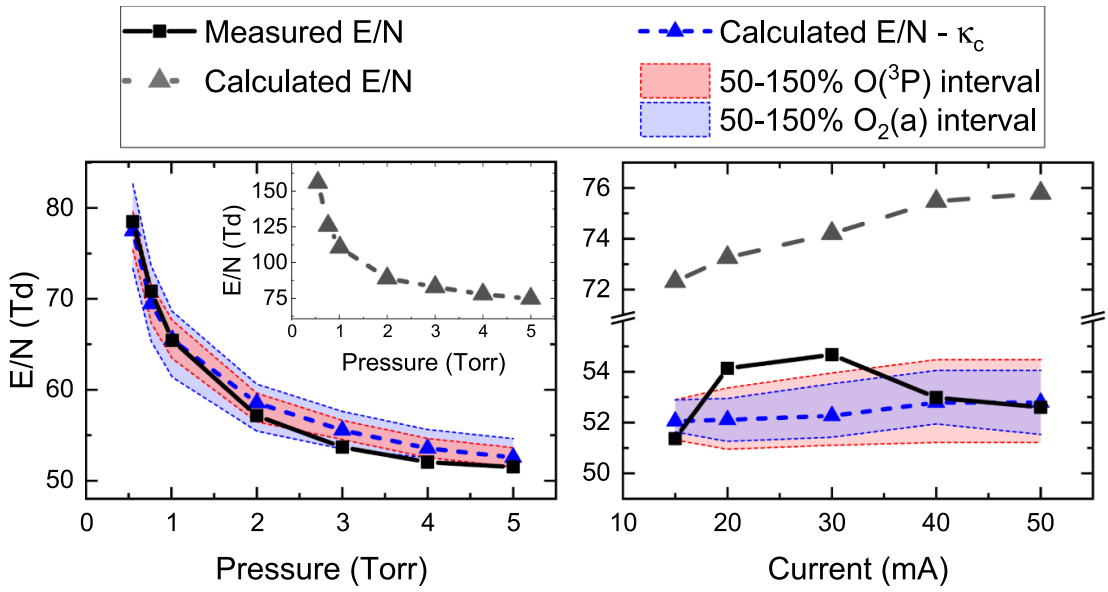

Figure 9. Results of the calculation of the reduced electric field using the line-ratio method with the Ar750 and Xe828 lines. Pressure variation running at 40 mA current (left) and current variation at 5 Torr (right). Results in blue include the correction factor $\kappa_{c,Ar} = 3$. Shaded areas show a 50%–150% interval of the $O(^3P)$ and $O_2(a)$ populations. Experimental conditions are those presented in figure 2. $O_2(a)$ population is taken from [13].

Ar line intensities need to be corrected by a factor of 3 (see figure 7 and its discussion). Using the correction factor $\kappa_{c,Ar} = 3$ based on the direct line intensity calculations, the results are shown to agree very well both in trend over pressure and current, and in absolute value, as seen in the blue dashed line. The apparent deviation of the measured E/N for the current variation at 20 and 30 mA is limited to a few Townsend (less than 5% of the reduced field), and likely stems from experimental error.

These results were obtained using the measured values of the atomic oxygen density (by CRDS, in figure 2) and literature values of the $O_2(a)$ density [13] in the EEDF calculation. In other circumstances, atomic oxygen density measurements may not be available. Therefore, we tested the sensitivity of our method to $[O(^3P)]$. The blue shaded area shows how the obtained value of E/N varies as the atomic oxygen density is varied over the range 50%–150%. This results in a difference of less than 7% in the estimated E/N. Similarly, the sensitivity to the $O_2(a)$ population is tested. The red shaded area shows the effect of varying the $O_2(a)$ population over the interval 50%–150%, compared to the values given in the literature [13]. A maximum difference of 3.5% in E/N is found.

Figure 10 shows the ratio of the excitation rate coefficients k_{Ar750}/k_{Xe828}, for different $O(^3P)$ and $O_2(a)$ input values. The correction factor for the argon excitation rate coefficient is included. An increase of either $O(^3P)$ or $O_2(a)$ will decrease the reduced electric field for a given ratio of rate coefficients. However, the sensitivity of the method to these input values is relatively small; an increase in the mole fraction of $O(^3P)$ or $O_2(a)$ by 0.1 gives a difference of only 2–3 Td.

Since the chemistry and electron kinetics are not resolved self-consistently, this sensitivity to the $O_2(a)$ and atomic oxygen densities derives solely from the changes these species introduce in the EEDF: For a larger atomic oxygen density, the mean free path of the electrons increases, increasing the tail of the EEDF. Changes in the $O(^3P)$ density can also impact the quenching term as the gas composition changes, but this effect is smaller than that associated with changes in the EEDF. Overall, a higher $O(^3P)$ fraction lowers the estimated reduced electric field. For $O_2(a)$, a larger population will increase the tail of the EEDF due to super-elastic collisions and, accordingly, will lead to a decrease in the calculated E/N. Importantly, the effect of $[O_2(a)]$ and $[O(^3P)]$ on electronegativity and electron production (i.e. through detachment processes) are not considered in our analysis. A complete evaluation of the chemistry and electron kinetics of O_2 plasmas and more details on the effect of $O_2(a)$ and $O(^3P)$ can be found in Dias *et al* [51].

Using figure 10 allows for a more direct implementation of the line ratio method: By calculating k_{Ar750}/k_{Xe828} using (5), the reduced electric field value can be found using the curves in the figure. Knowledge on the $O(^3P)$ and $O_2(a)$ mole fractions will enhance the precision of the E/N determination. The data from figure 10 is tabulated in the supplementary information, including more combinations

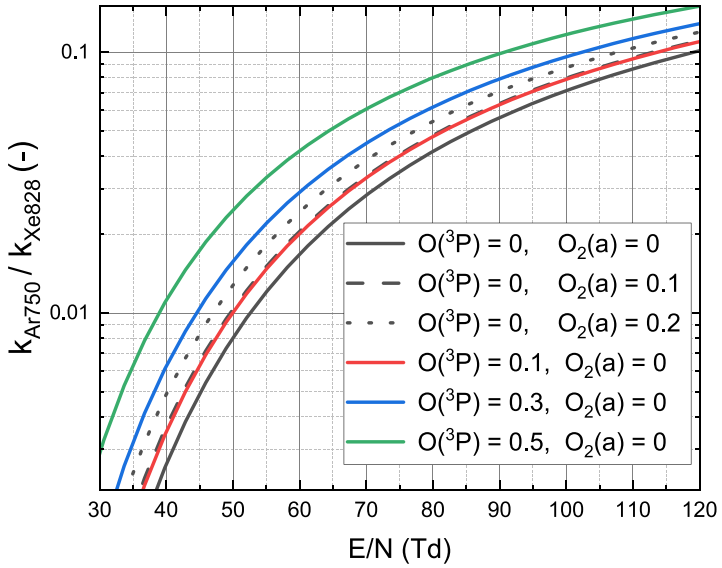

Figure 10. The sensitivity of the ratio of excitation rate coefficients, k_{Ar750}/k_{Xe828}, to the $O(^3P)$ and $O_2(b)$ mole fractions. The correction factor for the argon rate coefficients, $\kappa_{c,Ar} = 3$, is included.

of the $O(^3P)$ and $O_2(a)$ mole fractions. It can provide a useful tool for E/N determination without the need of the implementation of the Boltzmann solver.

The results of varying the density of $O_2(a)$ or $O(^3P)$ by 50%–150% in figure 9 show that the method is rather insensitive to these values, with maximum deviation in estimated E/N of 7%. This indicates that using estimated or literature values if measured $O_2(a)$ or $O(^3P)$ densities are unavailable will have a low impact on the calculated E/N value. However, this conclusion cannot be generalized to the use of other line ratios like Ar750/Ar811 or O845/O777, because their accuracy will mostly be limited by the ratio of excitation rate coefficients as shown in figure 8. One should note that the temperature and the atomic oxygen density from CRDS measurements are radially localized values, corresponding to the radially centered beam path of the CRDS beam, where both the atomic oxygen density fraction and the gas temperature are the highest [11, 13, 51]. The calculated reduced electric field is thus also a local value. A correction of the reduced electric field to a global value can easily be done if an average gas density or temperature is known and a radially homogeneous electric field is assumed.

Both the calculated reduced electric field and the atomic oxygen density are shown to be in excellent agreement with direct measurements when the correction factor for the argon cross section is included. An underestimation of the amplitude of the excitation cross sections of argon from [53] is thus strongly implied. However, to the knowledge of the authors, none of the argon cross sections in literature would have an amplitude large enough to both account for this correction, and reproduce the trends over pressure and current accurately (a comparison of the many relevant cross sections available is presented in part I [1]). The trends over pressure and current variation for both the reduced electric field (this work) and atomic oxygen density (part I) are very well reproduced using the cross sections from [52, 53] with our suggested correction factor $\kappa_{c,Ar} = 3$. However, an alternative explanation for our observations could be inaccuracies in the calculated EEDF, specifically an underestimation of the density of electrons with energy above 13.5 eV that can excite Ar. This could be caused by inaccuracies in the cross-section set used in the Boltzmann equation, notably with an underestimation of the inelastic cross-sections in the energy region above 13.5 eV. A similar inaccuracy in the high-energy tail of the calculated EEDF in O_2 was also invoked by Talviste *et al* [69] to explain discrepancies with their experimental observations. From the current analysis this cannot be determined, and thus further studies are required to clarify this question.

The values of the reduced electric field determined using different line ratios is shown in figure 11. The correction factor for the argon cross section is included in the calculations. The best results are found for the argon–xenon line ratio, but satisfactory results are also obtained using the argon-oxygen line ratio, with only a slight underestimation of the reduced electric field for the pressure and current variations under investigation. However, other combinations of lines (also presented in figure 8) were found to yield significantly incorrect values for E/N, due to insensitivity of the ratio of rate coefficients to E/N (in the range studied here, for lower E/N these line ratios might be effective), as only a small

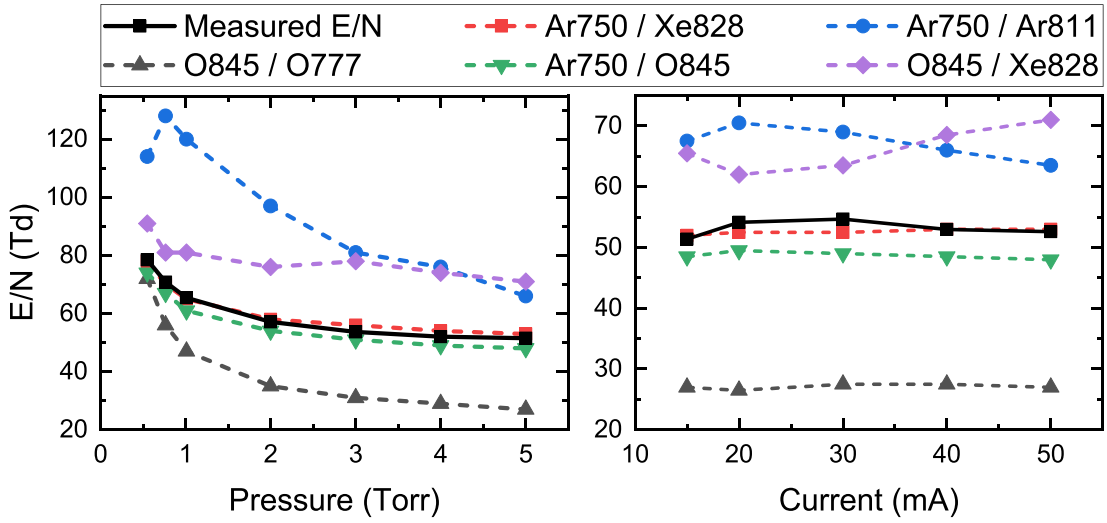

Figure 11. Results of the calculation of the reduced electric field using the line-ratio method using different line ratios, including the correction factor $\kappa_{c,Ar} = 3$. Pressure variation running at 40 mA current (left) and current variation at 5 Torr (right). Experimental conditions are those presented in figure 2. $O_2(a)$ population is taken from [13].

section of the tail of the EEDF is probed because the excitation thresholds of the two lines are similar. Use of the oxygen-argon line ratio is a reasonable option when the addition of xenon is not possible. It does, however, introduce an additional error in E/N from the uncertainty in the atomic oxygen density. Moreover, while spatial distributions for atomic oxygen and the trace gases are similar in our discharge due to the use of a Pyrex tube with low O atom loss probability [11], for other types of discharges, the spatial gradient of densities is to be considered, and, for example, tomographic methods such as an Abel inverse could be applied to obtain spatial resolution.

5. Conclusions

A method is proposed to estimate the reduced electric field in oxygen DC glow discharges from emission line ratios, based on calculations of the EEDF using the Boltzmann solver LoKI-B and an extended corona model, and using input data validated for atomic oxygen actinometry presented in part I [1]. The reduced electric field is investigated in discharges over a pressure variation of 0.55–5 Torr running at 40 mA current and for a current variation of 15–50 mA running at 5 Torr. The values obtained are in good agreement with E/N measured directly using electric field probes and the gas temperature measured by CRDS.

The electron impact excitation cross sections of [52, 53] are used. They were selected in part I [1] based on the reproduction of the trend of the emission line intensities over a range of E/N (through pressure variation) and give excellent agreement in terms of trends over pressure and current for both the atomic oxygen density (presented in part I, [1]), and the reduced electric field (this work).

A relative correction of the electron impact excitation cross sections of argon is necessary to get good agreement for the magnitude of the line intensity calculations for the argon emission lines. The value of the correction factor is determined to be $\kappa_c = 3 \pm 0.5$. Including this correction, both the trend over pressure and the intensity of the line intensities are in very good agreement with the experimentally retrieved values.

Using the line ratio method with xenon and argon line intensities, together with other inputs and the correction factor as described, the reduced electric can be estimated accurately. The values are in good agreement with direct measurements, both in absolute value and trends with pressure and current. The sensitivity to the densities of $O(^3P)$ and $O_2(a)$ is tested by varying these values in the calculations from 50%–150%. The calculated E/N was found to be only weakly sensitive to these input values, as a difference of less than 7% is induced. The method therefore can give a reasonable estimation of the reduced electric field even without actively probing the discharge composition. The results were validated for E/N of 50 to 80 Td.

The accurate reproduction of E/N and the atomic oxygen density using the methods presented in these combined works, including the correction factor for the argon cross sections, implies an underestimation of the amplitude of the argon cross sections. However, it should be noted that the mismatch in

line intensity calculations could also be the result of inaccurate EEDF estimation in the range above the threshold value of the argon emission lines (13 eV), due to inaccuracy of the cross-section sets. Further investigation is recommended.

The optimal emission lines to use depend upon the exact discharge probed: the difference in excitation threshold energy must be comparable to the electron temperature. In the case presented here, the preferred lines are Ar and Xe emission lines emitting at 750 and 828 nm respectively. Both are added as trace gases. The ratio of ground state densities is thus known and constant. Alternatively, one of the atomic oxygen triplets emitting at 777 or 845 nm can be used with the argon emission line at 750 nm. Note, however, that this method additionally requires estimation of the density of atomic oxygen.

In future work validation in a CO_2 discharge would extend the use of the method. The method presented here, combined with actinometry as presented in part I [1] can be a powerful tool for determining atomic oxygen density and reduced electric field in discharges in an easy and cheap manner without perturbing the discharge.

Data availability statement

The data cannot be made publicly available upon publication because the cost of preparing, depositing and hosting the data would be prohibitive within the terms of this research project. The data that support the findings of this study are available upon reasonable request from the authors.

Supplementary Data for Part II, Electric field measurements available at https://doi.org/10.1088/1361-6595/ae24aa/data1.

Acknowledgments

IPFN activities were funded by FCT (Fundação para a Ciência e a Tecnologia) under Projects UIDB/50010/2020 (https://doi.org/10.54499/UIDB/50010/2020), UIDP/50010/2020 (https://doi.org/10.54499/UIDP/50010/2020), LA/P/0061/2020 (https://doi.org/10.54499/LA/P/0061/2020) and PTDC/FIS-PLA/1616/2021 (https://doi.org/10.54499/PTDC/FIS-PLA/1616/2021).

ORCID iDs

L Kuijpers 0009-0000-6369-3674
E Baratte 0009-0009-8783-3446
O Guaitella 0000-0002-6509-6934
J-P Booth 0000-0002-0980-3278
V Guerra 0000-0002-6878-6850
M C M van de Sanden 0000-0002-4119-9971
T Silva 0000-0001-9046-958X

References

[1] Baratte E, Kuijpers L, Silva T, Guerra V, van de Sanden R, Booth J-P and Guaitella O 2025 Determination of the accuracy of actinometry and line ratio techniques in an O_2 glow discharge: part I, comparison of absolute oxygen atom densities with CRDS measurements *Plasma Sources Sci. Technol.* (https://doi.org/10.1088/1361-6595/ae24a9)
[2] Snoeckx R and Bogaerts A 2017 Plasma technology-a novel solution for CO_2 conversion? *Chem. Soc. Rev.* **46** 5805–63
[3] Rouwenhorst K H R, Jardali F, Bogaerts A and Lefferts L 2021 From the Birkeland-Eyde process towards energy-efficient plasma-based NOx synthesis: a techno-economic analysis *Energy Environ. Sci.* **14** 2520–34
[4] George S M 2010 Atomic layer deposition: an overview *Chem. Rev.* **110** 111–31
[5] Kanarik K J, Lill T, Hudson E A, Sriraman S, Tan S, Marks J, Vahedi V and Gottscho R A 2015 Overview of atomic layer etching in the semiconductor industry *J. Vac. Sci. Technol. A* **33** 020802
[6] Moon I J and Won C H 2018 Review of the current state of medical plasma technology and its potential applications *Med. Lasers* **7** 1–5
[7] Adamovich I *et al* 2022 The 2022 Plasma Roadmap: low temperature plasma science and technology *J. Phys. D: Appl. Phys.* **55** 373001
[8] Hagelaar G J and Pitchford L C 2005 Solving the Boltzmann equation to obtain electron transport coefficients and rate coefficients for fluid models *Plasma Sources Sci. Technol.* **14** 722–33
[9] Tejero-Del-Caz A, Guerra V, Gonçdiialves D, Silva M L D, Marques L, Pinhão N, Pintassilgo C D and Alves L L 2019 The LisbOn KInetics Boltzmann solver *Plasma Sources Sci. Technol.* **28** 043001
[10] Dias T C, Caz A T-del, Alves L L and Guerra V 2023 The LisbOn KInetics Monte Carlo solver *Comput. Phys. Commun.* **282** 108554
[11] Booth J P, Guaitella O, Chatterjee A, Drag C, Guerra V, Lopaev D, Zyryanov S, Rakhimova T, Voloshin D and Mankelevich Y 2019 Oxygen (^{3}P) atom recombination on a Pyrex surface in an O_2 plasma *Plasma Sources Sci. Technol.* **28** 055005
[12] Booth J P *et al* 2022 Quenching of $O_2(b^1\Sigma_g^+)$ by $O(^3P)$ atoms. Effect of gas temperature *Plasma Sources Sci. Technol.* **31** 065012
[13] Booth J *et al* 2020 Determination of absolute $O(^3P)$ and $O_2(a^1\Delta_g)$ densities and kinetics in fully modulated O_2 DC glow discharges from the $O_2(X^3\Sigma_g^-)$ afterglow recovery dynamics *Plasma Sources Sci. Technol.* **29** 115009

[14] Morillo-Candas A S, Drag C, Booth J-P, Dias T C, Guerra V and Guaitella O 2019 Oxygen atom kinetics in CO_2 plasmas ignited in a DC glow discharge *Plasma Sources Sci. Technol.* **28** 075010
[15] Adamovich I, Butterworth T, Orriere T, Pai D Z, Lacoste D A and Cha M S 2020 Nanosecond second harmonic generation for electric field measurements with temporal resolution shorter than laser pulse duration *J. Phys. D: Appl. Phys.* **53** 145201
[16] Chng T L, Starikovskaia S M and Schanne-Klein M C 2021 Electric Field Measurements in Plasmas with E-FISH Using Focused Gaussian Beams *2021 Conf. on Lasers and Electro-Optics Europe and European Quantum Electronics Conf., CLEO/Europe-EQEC 2021* (Institute of Electrical and Electronics Engineers Inc) (https://doi.org/10.1109/CLEO/Europe-EQEC52157.2021.9542435)
[17] Goldberg B M, Chng T L, Dogariu A and Miles R B 2018 Electric field measurements in a near atmospheric pressure nanosecond pulse discharge with picosecond electric field induced second harmonic generation *Appl. Phys. Lett.* **112** 064102
[18] Dogariu A, Goldberg B M, O'Byrne S and Miles R B 2017 Species-Independent Femtosecond Localized Electric Field Measurement *Phys. Rev. Appl.* **7** 024024
[19] Engeln R, Klarenaar B and Guaitella O 2020 Foundations of optical diagnostics in low-temperature plasmas *Plasma Sources Sci. Technol.* **29** 063001
[20] Fiebrandt M, Hillebrand B, Spiekermeier S, Bibinov N, Böke M and Awakowicz P 2017 Measurement of Ar resonance and metastable level number densities in argon containing plasmas *J. Phys. D: Appl. Phys.* **50** 355202
[21] Laux C, Spence T G, Kruger C H and Zare R N 2003 Optical diagnostics of atmospheric pressure air plasmas *Plasma Sources Sci. Technol* **12** 125–38
[22] Bruggeman P J, Sadeghi N, Schram D C and Linss V 2014 Gas temperature determination from rotational lines in non-equilibrium plasmas: A review *Plasma Sources Sci. Technol.* **23** 023001
[23] Onishi H, Yamazaki F, Hakozaki Y, Takemura M, Nezu A and Akatsuka H 2021 Measurement of electron temperature and density of atmospheric-pressure non-equilibrium argon plasma examined with optical emission spectroscopy *Jpn. J. Appl. Phys.* **60** 026002
[24] Zhu X-M and Pu Y-K 2010 Optical emission spectroscopy in low-temperature plasmas containing argon and nitrogen: Determination of the electron temperature and density by the line-ratio method *J. Phys. D: Appl. Phys.* **43** 403001
[25] Greb A, Niemi K, O'Connell D and Gans T 2014 Energy resolved actinometry for simultaneous measurement of atomic oxygen densities and local mean electron energies in radio-frequency driven plasmas *Appl. Phys. Lett.* **105** 234105
[26] Tsutsumi T, Greb A, Gibson A R, Hori M, O'Connell D and Gans T 2017 Investigation of the radially resolved oxygen dissociation degree and local mean electron energy in oxygen plasmas in contact with different surface materials *J. Appl. Phys.* **121** 143301
[27] Steuer D, Van Impel H, Gibson A R, Gathen V S-V D, Böke M and Golda J 2022 State enhanced actinometry in the COST microplasma jet *Plasma Sources Sci. Technol.* **31** 10LT01
[28] Donnelly V M 2004 Plasma electron temperatures and electron energy distributions measured by trace rare gases optical emission spectroscopy *J. Phys. D: Appl. Phys.* **37** R217
[29] Pagnon D, Amorim J, Nahorny J, Touzeau M and Vialle M 1995 On the use of actinometry to measure the dissociation in O_2 DC glow discharges: determination of the wall recombination probability *J. Phys. D: Appl. Phys.* **28** 1856–68
[30] Malyshev M V and Donnelly V M 1997 Determination of electron temperatures in plasmas by multiple rare gas optical emission and implications for advanced actinometry *J. Vac. Sci. Technol. A* **15** 550–8
[31] Donnelly V M, Malyshev M, Kornblit A, Ciampa N, Colonell J and Lee J 1998 Trace rare gases optical emission spectroscopy for determination of electron temperatures and species concentrations in chlorine-containing plasmas *Jpn. J. Appl. Phys.* **37** 2388–93
[32] Donnelly V M, Malyshev M V, Schabel M, Kornblit A, Tai W, Herman I P and Fuller N C M 2002 Optical plasma emission spectroscopy of etching plasmas used in Si-based semiconductor processing *Plasma Sources Sci. Technol.* **11** A26–30
[33] Donnelly V M and Schabel M J 2002 Spatially resolved electron temperatures, species concentrations and electron energy distributions in inductively coupled chlorine plasmas, measured by trace-rare gases optical emission spectroscopy *J. Appl. Phys.* **91** 6288–95
[34] Malyshev M V, Dorrlielly V M, Colonell J I and Samukawa S 1999 Plasma Diagnosis and Charging Damage *1999 4th Int. Symp. on Plasma Process-Induced Damage (IEEE Cat. No.* 99TH8395*)* pp 149–54
[35] Malyshev M V and Donnelly V M 1999 Trace rare gases optical emission spectroscopy: Nonintrusive method for measuring electron temperatures in low-pressure, low-temperature plasmas *Phys. Rev.* E **60** 6016–29
[36] Malyshev M V, Donnelly V M, Downey S W, Colonell J I and Layadi N 2000 Diagnostic studies of aluminum etching in an inductively coupled plasma system: Determination of electron temperatures and connections to plasma-induced damage *J. Vac. Sci. Technol. A* **18** 849–59
[37] Malyshev M V and Donnelly V M 2000 Diagnostics of chlorine inductively coupled plasmas. Measurement of electron temperatures and electron energy distribution functions *J. Appl. Phys.* **87** 1642–9
[38] Fuller N, Donnelly V M and Herman I P 2002 Electron temperatures of inductively coupled Cl_2-Ar plasmas *J. Vac. Sci. Technol. A* **20** 170–3
[39] Fuller N, Malyshev M, Donnelly V M and Herman I P 2000 Characterization of transformer coupled oxygen plasmas by trace rare gases-optical emission spectroscopy and Langmuir probe analysis *Plasma Sources Sci. Technol.* **9** 116–27
[40] Schabel M J, Donnelly V M, Cheung K P, Kornblit A, Layadi F J and Tai W 2001 TRG-OES Measurements of Electron Temperatures During Fluorocarbon Plasma Etching of SiO_2 Damage Test Wafers *2001 6th Int. Symp. on Plasma- and Process-Induced Damage (IEEE Cat. No.* 01TH8538*)* pp 60–63
[41] Schabel M J, Donnelly V M, Kornblit A and Tai W W 2002 Determination of electron temperature, atomic fluorine concentration and gas temperature in inductively coupled fluorocarbon/rare gas plasmas using optical emission spectroscopy *J. Vac. Sci. Technol. A* **20** 555–63
[42] Boivin S, Glad X, Latrasse L, Sarkissian A and Stafford L 2018 Probing suprathermal electrons by trace rare gases optical emission spectroscopy in low pressure dipolar microwave plasmas excited at the electron cyclotron resonance *Phys. Plasmas* **25** 093511
[43] Chen Z , Donnelly V M, Economou D J, Chen L, Funk M and Sundararajan R 2009 Measurement of electron temperatures and electron energy distribution functions in dual frequency capacitively coupled CF4/O2 plasmas using trace rare gases optical emission spectroscopy *J. Vac. Sci. Technol.* A **27** 1159–65
[44] Stafford L, Khare R, Donnelly V M, Margot J and Moisan M 2009 Electron energy distribution functions in low-pressure oxygen plasma columns sustained by propagating surface waves *Appl. Phys. Lett.* **94** 021503
[45] Mattei S, Boudreault O, Khare R, Stafford L and Donnelly V M 2011 Characterization of a low-pressure chlorine plasma column sustained by propagating surface waves using phase-sensitive microwave interferometry and trace-rare-gas optical emission spectroscopy *J. Appl. Phys.* **109** 113304
[46] Behringer K 1991 Diagnostics and modelling of ECRH microwave discharges *Plasma Phys. Control. Fusion* **33** 997–1028

[47] Behringer K and Fantz U 1994 Spectroscopic diagnostics of glow discharge plasmas with non-Maxwellian electron energy distributions *J. Phys. D: Appl. Phys* **27** 2128–35
[48] Boffard J B, Lin C C and DeJosephJr C A 2004 Application of excitation cross sections to optical plasma diagnostics *J. Phys. D: Appl. Phys.* **37** R143–61
[49] Obrusnik A, Bilek P, Hoder T, Šimek M and Bonaventura Z 2018 Electric field determination in air plasmas from intensity ratio of nitrogen spectral bands: I. sensitivity analysis and uncertainty quantification of dominant processes *Plasma Sources Sci. Technol.* **27** 085013
[50] Tejero-Del-Caz A, Guerra V, o N P, Pintassilgo C D and Alves L L 2021 On the quasi-stationary approach to solve the electron Boltzmann equation in pulsed plasmas *Plasma Sources Sci. Technol.* **30** 065008
[51] Dias T C, Fromentin C, Alves L L, Tejero-Del-Caz A, Silva T and Guerra V 2023 A reaction mechanism for O_2 plasmas *Plasma Sources Sci. Technol.* **32** 084003
[52] Tayal S S and Zatsarinny O 2016 B-spline R-matrix-with-pseudostates approach for excitation and ionization of atomic oxygen by electron collisions *Phys. Rev. A* **94** 042707
[53] Zatsarinny O and Bartschat K 2013 The *B*-spline *R*-matrix method for atomic processes: application to atomic structure, electron collisions and photoionization *J. Phys. B: At. Mol. Opt. Phys.* **46** 112001
[54] Niemi K, Gathen V S-V D and Döbele H F 2005 Absolute atomic oxygen density measurements by two-photon absorption laser-induced fluorescence spectroscopy in an RF-excited atmospheric pressure plasma jet *Plasma Sources Sci. Technol.* **14** 375–86
[55] Sadeghi N, Setser D W, Francis A, Czarnetzki U and Döbele H F 2001 Quenching rate constants for reactions of Ar($4p'_0$, $4p_0$, $4p_2$ and $4p_2$) atoms with 22 reagent gases *J. Chem. Phys.* **115** 3144–54
[56] Xu J, Setser D W and Ku J K 1986 Xenon Oxide and Xenon Sulfide Emission Systems at 234 and 227 nm *Chem. Phys. Lett.* **132** 427–36
[57] Kramida A, Ralchenko Y and Reader J Team NISTASD 2022 *Nist Atomic Spectra Database* (https://doi.org/10.18434/T4W30F)
[58] Alves L 2014 The IST-Lisbon database on LXCat *J. Phys.: Conf. Ser.* **565** 012007
[59] Biagi S 2011 Fortran program MAGBOLTZ 8.97 (available at: www.lxcat.net)
[60] Caplinger J E and Perram G P 2020 The importance of cascade emission and metastable excitation in modeling strong atomic oxygen lines in laboratory plasmas *Plasma Sources Sci. Technol.* **29** 015011
[61] Pitchford L C *et al* 2017 LXCat: an open-access, web-based platform for data needed for modeling low temperature plasmas *Plasma Process. Polymers* **14** 1600098
[62] Navrátil Z, Kusýn L, Prokop D and Hoder T 2025 On the Ar I 419.8 nm/751.5 nm (3p5/2p5) line intensity ratio for electric field measurement in dielectric barrier discharge in argon at atmospheric pressure *Plasma Sources Sci. Technol.* **34** 015013
[63] Chilton J E, Boffard J B, Schappe R S and Lin C C 1998 Measurement of electron-impact excitation into the 3p 5 4p levels of argon using Fourier-transform spectroscopy *Phys. Rev. A* **57** 267–77
[64] King D L, Piper L G and Setser D W 1977 Electronic energy transfer from metastable argon ($4s^3p_2, 0$) to xenon, oxygen and chlorine atoms *J. Chem. Soc. Faraday Trans.* **73** 177–200
[65] Velazco J E, Kolts J H and Setser D W 1978 Rate constants and quenching mechanisms for the metastable states of argon, krypton and xenon *J. Chem. Phys.* **69** 4357–73
[66] Kutasi K, Guerra V and Sá P 2010 Theoretical insight into Ar-O_2 surface-wave microwave discharges *J. Phys. D: Appl. Phys.* **43** 175201
[67] Luo L-Y, Donkó Z, Masheyeva R, Vass M, Li H-P and Hartmann P 2025 The quenching effect of oxygen addition on an argon capacitively coupled plasma: experimental and computational study of the argon metastable atom kinetics *Plasma Sources Sci. Technol.* 34 015009
[68] Fiebrandt M, Bibinov N and Awakowicz P 2025 Determination of atomic oxygen state densities in a double inductively coupled plasma using optical emission and absorption spectroscopy and probe measurements *Plasma Sources Sci. Technol.* **29** 045018
[69] Talviste R *et al* 2022 Effective ionization coefficient in mixtures of ar and O_2 determined using the townsend discharge *AIP Adv.* **12** 105213